Diffraction and the study of aqua ions

ARTICLE *in* THE JOURNAL OF PHYSICAL CHEMISTRY · NOVEMBER 1987

Impact Factor: 2.78 · DOI: 10.1021/j100307a008 · Source: OAI

FEATURE ARTICLE

Diffraction and the Study of Aqua Ions

J. E. Enderby,*† S. Cummings,‡ G. J. Herdman,§ G. W. Neilson,§ P. S. Salmon,∥ and N. Skipper§

Institut Laue-Langevin, 38042 Grenoble, France, Schuster Laboratory, University of Manchester, Manchester M13 9PL, U.K., H. H. Wills Physics Laboratory, University of Bristol, Bristol BS8 1TL, U.K., and School of Mathematics and Physics, University of East Anglia, Norwich NR4 7TJ, U.K.
(Received: June 4, 1987)

The method of differences as applied to neutron and X-ray diffraction studies of aqueous solutions is described. It is shown how detailed characterization of aqua ions in solution is made possible by the method; three topics (the comparison between crystal hydrates and concentrated solutions, the transition from the dilute solution regime to that of the molten salt, and the incomplete hydration of cations in solution) are chosen for detailed discussion.

1. Introduction

"The logical place to begin a discussion of the formation and stability of complex ions in aqueous solutions is with the aqueous ions themselves .... If we regard the [metal] ion as being an aqueous complex $[M(H_2O)_n]^{p+}$, which is then further and more loosely solvated, we wish to know the coordination number n and also the manner in which the n molecules are arranged around the metal ion."[1] These two sentences, taken from Cotton and Wilkinson's *Advanced Inorganic Chemistry*, a textbook of quite outstanding clarity and insight, form an admirable starting point to this article.

We therefore begin by considering the *partial radial distribution* function $g_{\alpha\beta}(r)$ which measures the probability of finding a β-type particle at a distance r from an α-type particle placed at the origin. In order to understand this in a quantitative fashion, let us consider an α-type particle at the origin and ask what is the average number of β-type particles that occupy a spherical shell of radius r and thickness dr at the same instant of time. That number is given by

$$dn_{\alpha\beta} = 4\pi\rho_\beta g_{\alpha\beta}(r) r^2\, dr \qquad (1)$$

where $\rho_\beta = N_\beta/V$ and N_β is the number of β species contained in the sample of volume V.

In Figure 1a we sketch a hypothetical $g_{MO}(r)$ for an aqueous solution consisting of a salt M_qX_p (M = cation of valence p; X = anion of valence q) dissolved in H_2O. Let us focus attention on the parameters indicated on the sketch. The chance of finding the ion M^{p+} and the oxygen atom separated by a distance less than r_c is negligible. Thus, r_c measures the closest distance of approach of M and O in the system. On the other hand, the value of $\bar{r}_{MO}$ allows us to define the most probable separation and r_d tells us the spatial extent of the short-range MO interactions. The values of $g_{MO}(r)$ with r equal to $\bar{r}_{MO}$ and r_d are denoted h and h', respectively. It follows from the definition of $g_{\alpha\beta}(r)$ given in eq 1 that the value of the integral

$$4\pi\rho_0 \int_0^{r_s} g_{MO}(r) r^2\, dr$$

is the running coordination number, i.e., the average number of oxygen atoms within a spherical shell of radius r_s for a metal ion chosen to be at the origin. If r_s is chosen as r_d, this value of the running coordination number is usually referred to as the *hydration number*, which we will write in a generalization of the Cotton–Wilkinson notation as $\bar{n}_{MO}$. Although the ratio h'/h is typically $\sim 1/4$ for simple liquids, it tends to zero for some ionic solutions, indicating that well-defined local order persists for times greater than $\sim 10^{-11}$ s. To put it in yet another way, small or zero values of h'/h are expected if the aqua ion forms a stable chemical complex. If comparable information is extracted from the M–H pair correlation function $g_{MH}(r)$ (Figure 1b), further structural and electrochemical information is made available. For example, from the values of $\bar{r}_{MO}$ and $\bar{r}_{MH}$ it is possible to deduce the mean angle of tilt θ shown in Figure 1c. A comparison of $\bar{n}_{MO}$ and $\bar{n}_{MH}$ can reveal the extent to which the aqua ion is acidic, since the dissociation

$$[M(H_2O)_n]^{p+} \rightleftharpoons [M(H_2O)_{n-1}(OH)]^{(p-1)+} + H^+$$

will lead to $\bar{n}_{MH} < 2\bar{n}_{MO}$. In practice, only strongly acidic behavior (e.g., Fe^{3+}) has been detected because of the errors in the determination of $\bar{n}$.

2. Diffraction Theory

In order to determine $g_{\alpha\beta}(r)$ experimentally, we must link this quantity with the results of diffraction theory. If neutrons or X-rays are incident on a liquid containing several chemical species, a measure of the amplitude of the scattered waves is given by

$$\sum_\alpha b_\alpha \sum_{i(\alpha)} \exp[i\mathbf{k}\mathbf{r}_i(\alpha)] \qquad (2)$$

where b_α is the mean neutron coherent scattering length in neutron scattering [or the X-ray form factor in X-ray scattering, usually written $f_\alpha(k)$] and $\mathbf{r}_i(\alpha)$ denotes the position of the ith nucleus of the α-type. In eq 2 the second sum looks after the phase relationships of the waves scattered from the nuclei at different positions. The sum over the α values, on the other hand, takes account of the different scattering lengths for the different kinds of nuclei or atoms. The intensity of coherently scattered radiation is given by

$$I(k) = \sum_\alpha \sum_\beta b_\alpha b_\alpha \sum_{i(\alpha)} \sum_{j(\beta)} \exp\{i\mathbf{k}[\mathbf{r}_j(\beta) - \mathbf{r}_i(\alpha)]\} \qquad (3)$$

and can in principle be obtained from an experimental setup such as that shown in Figure 2a. The quantity $\mathbf{k}$ is the scattering vector whose modulus, k, for elastic scattering (i.e., $|\mathbf{k}_0| = |\mathbf{k}_1|$) (see Figure 2b) is given by

$$k = 2k_0 \sin\theta$$

or, since $k_0 = 2\pi/\lambda_0$, $k = (4\pi \sin\theta)/\lambda_0$, where λ_0 is the incident wavelength and θ is half the scattering angle. To do diffraction

† Institut Laue-Langevin.
‡ University of Manchester.
§ University of Bristol.
∥ University of East Anglia.

(1) Cotton, F. A.; Wilkinson, G. *Advanced Inorganic Chemistry*, 3rd ed.; Wiley: New York, 1972.

0022-3654/87/2091-5851$01.50/0

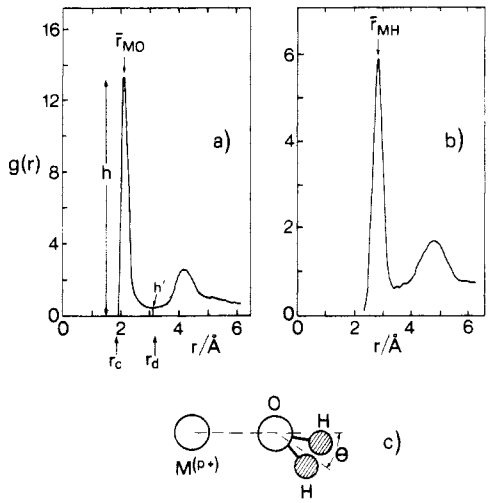

Figure 1. (a and b) Hypothetical radial distribution functions $g_{\alpha\beta}(r)$, $g_{MO}(r)$, and $g_{MH}(r)$ for an aqua ion in solution. (c) The geometry of an aqua ion.

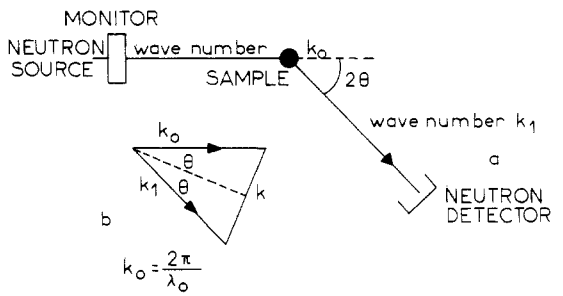

Figure 2. (a) Conventional arrangement for neutron diffraction studies. (b) The scattering triangle for elastic scattering: $|k_0| = |k_1|$.

experiments, an intense source of neutrons or X-rays is required. For neutrons this is normally a high-flux nuclear reactor, although pulsed sources based on nuclear spallation will play a major role in the future. X-rays can be derived from conventional laboratory sources or, if very high fluxes or tunability are required, synchrotron radiation.

Elementary manipulation of eq 3 yields an expression of the form

$$I(k) = N[\sum_{\alpha} c_\alpha b_\alpha^2 + F(k)] \quad (4)$$

where c_α is the atomic fraction of the α species, N is the total number of nuclei, and $F(k)$ is a weighted average of the *partial structure factors*, $S_{\alpha\beta}(k)$, whose Fourier transform yields $g_{\alpha\beta}(r)$. Explicitly

$$F(k) = \sum_{\alpha}\sum_{\beta} c_\alpha c_\beta b_\alpha b_\beta [S_{\alpha\beta}(k) - 1] \quad (5)$$

and

$$g_{\alpha\beta}(r) = 1 + \frac{1}{2\pi^2\rho r}\int [S_{\alpha\beta}(k) - 1]k \sin(kr)\, dk \quad (6)$$

where ρ is the total number density.

Four important points must now be made. First, the neutron scattering length is *isotropic*, i.e., it does not depend on k. It varies with isotope and with atomic number in an irregular manner. Examples of scattering lengths relevant to the study of aqueous solutions are shown in Table I. Second, the Fourier transform of $F(k)$

$$G(r) = \frac{1}{2\pi^2\rho r}\int F(k)k \sin(kr)\, dk \quad (7)$$

can, for the neutron case, be written as a *linear combination* of all the radial distribution functions, i.e.

$$G(r) = \sum_{\alpha}\sum_{\beta} c_\alpha c_\beta b_\alpha b_\beta [g_{\alpha\beta}(r) - 1] \quad (8)$$

TABLE I: Examples of Coherent Scattering Lengths (fm[a])

element on isotope	b	element on isotope	b	element on isotope	b
H	−3.74	^{40}Ca	4.9	^{65}Cu	11.1
D	6.67	^{44}Ca	1.8	Zn	5.686
^{6}Li	1.87	Fe	9.51	^{64}Zn	5.5
^{7}Li	−2.2	^{54}Fe	4.2	^{68}Zn	6.7
N	9.36	^{56}Fe	10.1	Ag	5.97
^{14}N	9.37	^{57}Fe	2.3	^{107}Ag	7.64
^{15}N	6.44	Ni	10.3	^{109}Ag	4.19
K	3.67	^{58}Ni	14.4	^{113}In	5.39
^{41}K	2.58	^{60}Ni	2.82	^{115}In	4.00
Cl	9.58	^{62}Ni	−8.7	Ba	5.07
^{35}Cl	11.7	^{64}Ni	−0.37	^{130}Ba	−3.6
^{37}Cl	3.1	Cu	7.718	^{137}Ba	6.82
Ca	4.9	^{63}Cu	6.7		

[a] 1 fm = 10^{-15} m.

$G(r)$ is usually referred to as the total radial distribution function. Third, the X-ray form factors $f_\alpha(k)$ are k-dependent and $f_\alpha(k = 0)$ increases with atomic number in a linear way. Thus, the total X-ray radial distribution function is not a linear combination of $g_{\alpha\beta}(r)$ since k-dependent form factors remain inside the integral of eq 7 and lead to a "convolution broadening" of some of the structural features. Fourth, the above analysis assumes that the scattering is entirely elastic. In practice, there is no elastic scattering from liquids, and although the corrections which must be applied to eq 3 to allow for this are negligible for X-rays, they are particularly large for neutrons. Such corrections, now generally known as the "Placzek" corrections, are difficult to handle for hydrogenous liquids but can, as shown by Soper et al.,[2] be eliminated to first order by the "method of differences" which we now consider.

3. The Method of Differences As Applied to Neutron Diffraction

$F(k)$ is, as we have seen, a weighted average of several partial structure factors; for aqueous solutions of the form M_qX_p in H_2O, 10 structure factors enter into $F(k)$. The difficulty in interpreting $F(k)$ or its Fourier transform $G(r)$ in terms of ion–water and ion–ion correlation functions arises because, even for concentrated solutions, they make minor contributions to the total scattering.

The neutron "first-order" different method[2-4] allows one to gain direct information about the detailed arrangement of the water molecules around the ions in aqueous solution. The quantity that is central to the method is the difference between the $F(k)$'s for two samples that are identical in all respects except that the isotopic state of the cation, M, or the anion, X, has been changed; this quantity, denoted $\Delta_M(k)$ or $\Delta_X(k)$, is the sum of four partial structure factors $S_{\alpha\beta}(k)$ usually weighted in such a way that only those relating to ion–water correlations are significant. Explicitly:

$$\Delta_M(k) = A_M[S_{MO}(k) - 1] + B_M[S_{MD}(k) - 1] + C_M[S_{MX}(k) - 1] + D_M[S_{MM}(k) - 1]$$

$$\Delta_X(k) = A_X[S_{XO}(k) - 1] + B_X[S_{XD}(k) - 1] + C_X[S_{MX}(k) - 1] + D_X[S_{XX}(k) - 1]$$

$$A_M = 2c_Mc_Ob_O(b_M - b'_M); \quad A_X = 2c_Xc_Ob_O(b_X - b'_X)$$

$$B_M = 2c_Mc_Db_D(b_M - b'_M); \quad B_X = 2c_Xc_Db_D(b_X - b'_X)$$

$$C_M = 2c_Mc_Xb_X(b_M - b'_M); \quad C_X = 2c_Xc_Mb_M(b_X - b'_X)$$

$$D_M = c_M^2(b_M^2 - b'^2_M); \quad D_X = c_X^2(b_X^2 - b'^2_X)$$

and b_O and b_D are the neutron coherent scattering amplitudes for oxygen and deuterium and b_M, b'_M, b_X, and b'_X are the mean

(2) Soper, A. K.; Neilson, G. W.; Enderby, J. E.; Howe, R. A. *J. Phys. C: Solid State Phys.* **1977**, *10*, 1793.
(3) Enderby, J. E.; Neilson, G. W. *Rep. Prog. Phys.* **1981**, *44*, 593.
(4) Enderby, J. E. *Annu. Rev. Phys. Chem.* **1983**, *34*, 155.

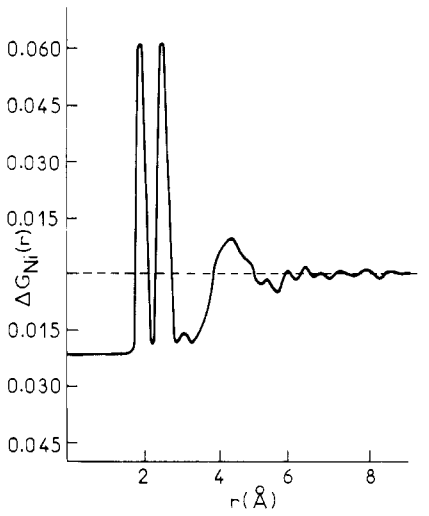

Figure 3. $\Delta G_{Ni}(r)$ in barns for a 1.46 *m* solution of $NiCl_2$ in D_2O. 1 b (barn) = 10^{-28} m^2.

scattering amplitudes for the isotopic states used in producing the salt M_qX_p. For neutron scattering, heavy water rather than light water is the preferred solvent, so D has replaced H in the subsequent analysis.

The properties of $\Delta(k)$ have been discussed in detail elsewhere (see especially ref 2) and need not be enlarged on here. The crucial property, apart from the fact that $A,B > C,D$ for solutions of molality less than ~5, is that Placzek distortions are essentially eliminated so that a difference function $\Delta G(r)$ can be determined directly from

$$\Delta G(r) = \frac{1}{2\pi^2\rho r}\int \Delta(k)k \sin(kr)\, dk$$

In terms of the correlation functions, $g_{\alpha\beta}(r)$, it follows at once that

$$\Delta G_M(r) = A_M[g_{MO}(r) - 1] + B_M[g_{MD}(r) - 1] + C_M[g_{MX}(r) - 1] + D_M[g_{MM}(r) - 1]$$

and

$$\Delta G_X(r) = A_X[g_{XO}(r) - 1] + B_X[g_{XD}(r) - 1] + C_X[g_{MX}(r) - 1] + D_X[g_{XX}(r) - 1]$$

Since A and B are much greater than C and D, the method yields a high-resolution measurement of an appropriate combination of $g_{MO}(r)$ and $g_{MD}(r)$ or $g_{XO}(r)$ and $g_{XD}(r)$. The contributions to $\Delta G(r)$ from the solvent terms alone, which normally dominate $G(r)$, have thus been totally eliminated by the difference method. We now have a way of investigating directly the various coordination complexes characteristic of aqueous solutions.

The "second-order" difference method[3] allows one to gain direct information about ion–ion correlations. The method requires *three* samples for $S_{MM}(k)$ or $S_{XX}(k)$ and *four* samples for $S_{MX}(k)$, and formulas for obtaining these functions are to be found in ref 3 and 4. In real space, the three ion–ion correlation functions can be obtained, once the $S_{\alpha\beta}(k)$ have been measured, by numerical integration of eq 6 with $\alpha, \beta = M$ or X.

4. Some Experimental Results

4.1. Cationic Hydration. We take as an illustrative example the Ni^{2+} aqua ion and show in Figure 3 $\Delta G_{Ni}(r)$ for a 1.46 *m* solution. This exhibits the twin peak structure characteristic of strongly hydrated ions and allows $\bar{r}_{MO}$ and $\bar{r}_{MD}$ (the mean ion–oxygen and ion–deuterium bond lengths), the hydration number, and the mean angle of tilt θ (see Figure 1c) to be determined. The stability of the aqua ion is reflected by the low value of h'/h and, as pointed out by Hunt and Friedman,[5] the data "decisively support the generally accepted stoichiometry for the complex". Comparable information is now available for several cations, and an up-to-date summary is given in Table II.

(5) Hunt, J. P.; Friedman, H. L. *Prog. Inorg. Chem.* **1983**, *30*, 359.

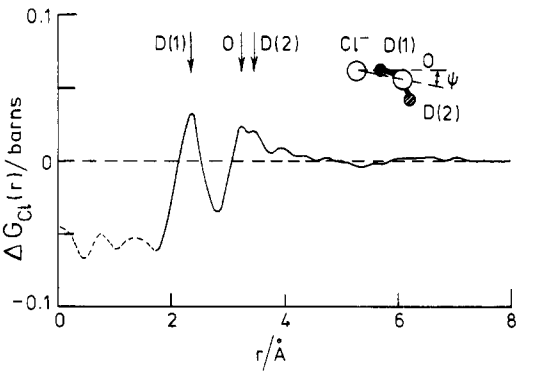

Figure 4. $\Delta G_{Cl}(r)$ for a 4.35 *m* solution of $NiCl_2$ in D_2O. 1 b (barn) = 10^{-28} m^2.

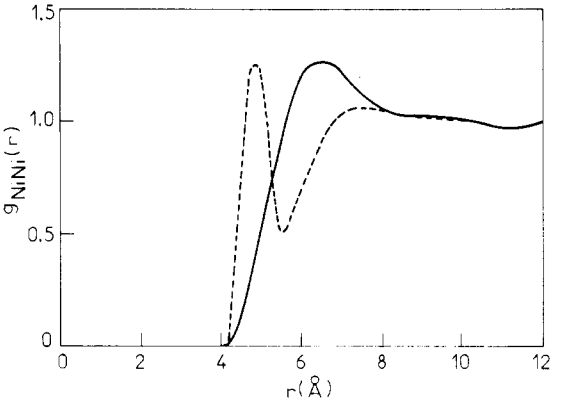

Figure 5. Radial distribution function $g_{NiNi}(r)$ for a 4.35 *m* solution of $NiCl_2$ in D_2O. Full curve: X-ray results. Dashed curve: neutron results.

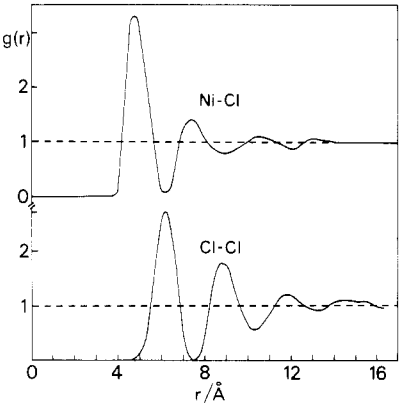

Figure 6. Radial distribution functions $g_{NiCl}(r)$ and $g_{ClCl}(r)$ for a 4.35 *m* solution of $NiCl_2$ in D_2O. The coordination numbers are 5.8 ± 0.3 (Cl^- around Ni^{2+}) and 8.5 ± 0.3 (Cl^- around Cl^-) respectively (see ref 22).

4.2. Anionic Hydration. Some years ago, Cummings et al.[6] found that the form of $\Delta G_{Cl}(r)$, for which Figure 4 is a typical

(6) Cummings, S.; Enderby, J. E.; Neilson, G. W.; Newsome, J. R.; Howe, R. A.; Howells, W. S.; Soper, A. K. *Nature (London)* **1980**, *287*, 714.
(7) Newsome, J. R.; Neilson, G. W.; Enderby, J. E. *J. Phys. C: Solid State Phys.* **1980**, *13*, L923.
(8) Ichikawa, K.; Kameda, Y.; Matsumoto, T.; Misawa, M. *J. Phys. C: Solid State Phys.* **1984**, *17*, L725.
(9) Neilson, G. W., private communication, 1986.
(10) Hewish, N. A.; Neilson, G. W. *Chem. Phys. Lett.* **1981**, *84*, 425.
(11) Hewish, N. A.; Neilson, G. W.; Enderby, J. E. *Nature (London)* **1982**, *297*, 138. Cummings, S.; Enderby, J. E.; Howe, R. A. *J. Phys. C: Solid State Phys.* **1980**, *13*, 1.
(12) Neilson, G. W.; Enderby, J. E. *J. Phys. C: Solid State Phys.* **1978**, *11*, L625.
(13) Newsome, J. R.; Neilson, G. W.; Enderby, J. E.; Sandström, M. *Chem. Phys. Lett.* **1981**, *82*, 399.
(14) Salmon, P. S. Ph.D. Thesis, University of Bristol, 1985.
(15) Salmon, P. S., private communication, 1986.

TABLE II: Cation Hydration at Room Temperature As Determined by Neutron Diffraction

ion	solute	molality	ion–oxygen dist, Å	ion–deuterium dist, Å	θ, deg	hydration no.	ref
Li^+	LiCl	27.77	1.95 ± 0.02	2.31 ± 0.02	75 ± 5	2.3 ± 0.2	
		9.95	1.95 ± 0.02	2.50 ± 0.02	52 ± 5	3.3 ± 0.5	7–9
		3.57	1.95 ± 0.02	2.55 ± 0.02	40 ± 5	5.5 ± 0.3	
ND_4^+	ND_4Cl	5.0	2.8–3.2	3.4–3.8		10.0–12.0	10
Ca^{2+}	$CaCl_2$	4.49	2.41 ± 0.03	3.04 ± 0.03	34 ± 9	6.4 ± 0.3[a]	
		2.80	2.39 ± 0.02	3.02 ± 0.03	34 ± 9	7.2 ± 0.2	11
		1.0	2.46 ± 0.03	3.07 ± 0.03	38 ± 9	10.0 ± 0.6	
Ni^{2+}	$NiCl_2$	4.41	2.07 ± 0.02	2.67 ± 0.02	42 ± 8	5.8 ± 0.2	
		3.05	2.07 ± 0.02	2.67 ± 0.02	42 ± 8	5.8 ± 0.2	
		1.46	2.07 ± 0.02	2.67 ± 0.02	42 ± 8	5.8 ± 0.3	12
		0.85	2.09 ± 0.02	2.76 ± 0.02	27 ± 10	6.6 ± 0.5	
		0.42	2.10 ± 0.02	2.80 ± 0.02	17 ± 10	6.8 ± 0.8	
		0.086	2.07 ± 0.03	2.80 ± 0.04	0 ± 20	6.8 ± 0.8	
Ni^{2+}	$Ni(ClO_4)_2$	3.80	2.07 ± 0.02	2.67 ± 0.02	42 ± 8	5.8 ± 0.2	13
Cu^{2+}	$CuCl_2$	4.32	1.96 ± 0.03	2.54 ± 0.03	45 ± 7	3.4 ± 0.3	14
Cu^{2+}	$Cu(ClO_4)_2$	2.00	1.96 ± 0.04			4.1 ± 0.3	15
Nd^{3+}	$NdCl_3$	2.85	2.48 ± 0.02	3.13 ± 0.02	24 ± 4	8.5 ± 0.2	16
Dy^{3+}	$DyCl_3$	2.38	2.37 ± 0.03	3.04 ± 0.03	17 ± 3	7.4 ± 0.5	17

[a] The hydration parameters listed here differ slightly from those quoted by Cummings et al. following a reevaluation of the original scattering data by Hewish et al. (ref 11).

TABLE III: Chloride Hydration at Room Temperature As Determined by Neutron Diffraction

ion	solute	molality	Cl^-–D(1), Å	Cl^-–O, Å	Cl^-–D(2), Å	Ψ, deg	coord no.	ref
Cl^-	LiCl	14.9	2.24 ± 0.02	3.25 ± 0.03	3.50–3.60	0	4.4 ± 0.3	
		9.95	2.22 ± 0.02	3.29 ± 0.04	3.50–3.68	0	5.3 ± 0.2	6, 18
		3.57	2.25 ± 0.02	3.34 ± 0.04	3.50–3.70	0	5.9 ± 0.2	
	NaCl	5.32	2.26 ± 0.03	3.20 ± 0.05		0–20	5.5 ± 0.4	
		3.62	2.25 ± 0.02	3.26 ± 0.03		0–10	5.7 ± 0.2	2, 19
	RbCl	4.36	2.26 ± 0.03	3.20 ± 0.05		0–20	5.8 ± 0.3	
	$CaCl_2$	4.49	2.25 ± 0.02	3.25 ± 0.04	3.55–3.65	0–7	5.8 ± 0.2	6, 18
	$NiCl_2$	4.35	2.29 ± 0.02	3.20 ± 0.04	3.40–3.50	5–11	5.7 ± 0.2	6, 18
	$NiCl_2$	3.00	2.23 ± 0.03	3.25 ± 0.05	3.40–3.50	0–8	5.5 ± 0.4	
	$CuCl_2$	4.32	2.27 ± 0.03	3.25 ± 0.05		0–7	3.3 ± 0.4	14
	$ZnCl_2$	45.1 (100 °C)	2.25 ± 0.05				1.0 ± 0.9	20
		19.4	2.25 ± 0.03	3.40 ± 0.2	3.7–3.9	0–7	1.9 ± 0.4	
		4.9	2.25 ± 0.03	3.40 ± 0.15	3.7–3.9	0–3	3.7 ± 0.5	
	$NdCl_3$	2.85	2.29 ± 0.02	3.45 ± 0.04		0	3.9 ± 0.2	21

example, was remarkably insensitive to the nature of the cation. This finding has been confirmed by many subsequent investigations, and a summary of the present experimental situation is given in Table III.

As the molten salt (high salt molality) region is approached, the hydration number generally falls from a value of about 6 as inner-sphere complexing between the anions and the cations becomes increasingly probable. From the data shown in Table III, it is evident that in some solutions the chloride hydration number can achieve a value close to 6 provided the H_2O/Cl^- ratio is itself ≥ 6. For other solutions, notably $ZnCl_2$ and $CuCl_2$, lower hydration numbers are found even at high H_2O/Cl^- ratios, which reflects the importance of inner-sphere complexing by the chloride ion and will, as we shall see, influence the form of the ion–ion distribution functions.

4.3. Ion–Ion Distribution Functions. Neilson and Enderby[22] determined $g_{NiNi}(r)$, $g_{NiCl}(r)$, and $g_{ClCl}(r)$ for a 4.35 *m* solution of $NiCl_2$ by the neutron method (Figures 5 and 6). The chloride–chloride distribution functions for solutions of LiCl[18] and $ZnCl_2$[20] have also been measured. These functions will be discussed in detail later in this paper.

5. Other Difference Methods for Aqueous Solutions

It is clear from what has been said already that the neutron method of differences is formally exact and is capable of yielding detailed structural information for aqueous solutions with precision. There are, however, three disadvantages in its practical implementation. First, it relies on the use of separated isotopes which are invariably expensive and sometimes not actually available in sufficient quantity for neutron work. Second, the experiments have to be performed at a central facility that can provide intense beams of thermal neutrons. The user pressure on these facilities is often so great that experiments may have to wait several months or even years before they can be tackled. Moreover, it is often difficult to justify, to the relevant allocation committee, a series of experiments that, by their nature, are time-consuming. For example, experiments in which the concentration of the additive is changed over a wide range in a systematic way would, if time were allocated, occupy long periods of machine time to the exclusion of other users.

Third, the variation of *b* that arises from isotopic substitution is ~20 fm in the most favorable case and is often considerably less (Table I). It follows that the second-order difference method developed to obtain ion–ion correlation functions is, with current technology, limited to relatively few solutions at concentrations in excess of ~3 *m*. The method Skipper et al.[23] have developed

(16) Narten, A. H.; Hahn, R. L. *Science (Washington, D.C.)* **1982**, *217*, 1249.
(17) Annis, B. K.; Hahn, R. L.; Narten, A. H. *J. Chem. Phys.* **1985**, *82*, 2806.
(18) Copestake, A.; Neilson, G. W.; Enderby, J. E. *J. Phys. C: Solid State Phys.* **1985**, *18*, 4211.
(19) Barnes, A. C.; Breen, J.; Lyte, J. C.; Enderby, J. E., unpublished results.
(20) Biggin, S. ISAS Report No. 16/86/CM; International Center for Theoretical Physics: Trieste, 1986; private communication.
(21) Biggin, S.; Enderby, J. E.; Hahn, R. L.; Narten, A. H. *J. Phys. Chem.* **1984**, *88*, 3634.
(22) Neilson, G. W.; Enderby, J. E. *Proc. R. Soc. London, A* **1983**, *390*, 353.
(23) Skipper, N. T.; Cummings, S.; Neilson, G. W.; Enderby, J. E. *Nature (London)* **1986**, *321*, 52.

to extract the required information makes use of *laboratory*-based X-ray diffraction and has three notable features. First it relies on *isomorphic* rather than *isotopic* substitution. In other words, $f_\alpha(k)$ is changed to $f_{\alpha'}(k)$ by replacing one element with another on the assumption that the set of structure factors $S_{\alpha\beta}(k)$ is unaffected. This is, of course, not new and has been tried by other workers, notably Bol et al.[24] for a range of aqueous solutions. The second feature concerns the way the difference function is treated.

Suppose that an isomorphic substitution has been satisfactorily made. Then the X-ray difference function $\tilde{\Delta}_\alpha(k)$ will be of the form

$$\tilde{\Delta}_\alpha(k) = 2c_\alpha\Delta f_\alpha(k)\sum_{\beta\neq\alpha} c_\beta f_\beta(k)[S_{\alpha\beta}(k) - 1] + c^2{}_\alpha[f^2{}_\alpha(k) - f^2{}_{\alpha'}(k)][S_{\alpha\alpha}(k) - 1]$$

where β labels all the chemical species other than the one isomorphically substituted, $\Delta f_\alpha(k) = f_\alpha(k) - f_{\alpha'}(k)$, and the tilde is used to differentiate the X-ray case from the neutron case. As in the neutron method, the structural effects due to the water are not present in the difference function and the systematic corrections (for example those due to Compton scattering) are greatly simplified. In order to eliminate the convolution broadening due to the k dependence of $f_\alpha(k)$, let us extract from the sum the term arising from a particular chemical species denoted by γ. Then

$$\tilde{\Delta}_\alpha(k) = 2c_\alpha c_\gamma\Delta f_\alpha(k)f_\gamma(k)[S_{\alpha\gamma}(k) - 1] + 2c_\alpha\Delta f_\alpha(k)\sum_{\beta\neq\gamma\neq\alpha} c_\beta f_\beta(k)[S_{\alpha\beta}(k) - 1] + c^2{}_\alpha[f^2{}_\alpha(k) - f^2{}_{\alpha'}(k)][S_{\alpha\alpha}(k) - 1]$$

The Fourier transform of $\tilde{\Delta}_\alpha(k)/2c_\alpha c_\gamma\Delta f_\alpha(k)f_\gamma(k)$, $\tilde{\Delta}G_\alpha(r)$, is of the form

$$\Delta\tilde{G}_\alpha(r) = [g_{\alpha\gamma}(r) - 1] + \sum_{\beta\neq\gamma} a_\beta\int H_\beta(|\mathbf{r} - \mathbf{r}'|)[g_{\alpha\beta}(\mathbf{r}') - 1]\,d\mathbf{r}'$$

where $H_\beta(|\mathbf{r} - \mathbf{r}'|)$ is a convolution function associated with the k dependence of the form factor and a_β are constants that can be evaluated for any pair of isomorphs. Provided that the first peak in $g_{\alpha\gamma}(r)$ is well separated from those of $g_{\alpha\beta}(r)$ ($\beta \neq \gamma$), a situation that normally obtains for well-coordinated ions, the isomorphic method, when treated in this way, yields an *unbroadened* pair correlation function, the choice of which is determined by γ. For example, if α represents a metal ion in solution and γ refers to oxygen, $\bar{r}_{MO}$ and $\bar{n}_{MO}$ can be measured.

The third feature of the new method is that one of the isomorphs should also show a neutron isotopic effect. This enables an *exact* $g_{\alpha\gamma}(r)$ to be obtained *via* neutron scattering so that a detailed comparison can be made between it and the $g_{\alpha\gamma}(r)$ derived from the X-ray method in the neighborhood of the first peak. Nonisomorphism will in general produce broadening in the real-space X-ray distribution function, and comparison with the neutron measurement enables the deviation from ideal isomorphic behavior to be quantified. Once isomorphism has been established, the time-consuming but scientifically significant studies involving changes in concentration, temperature, etc. can all be carried out in the laboratory without recourse to central facilities.

It is the combination of these three features that makes this approach to the study of aqueous solution by isomorphic substitution novel and represents a significant advance on what has been tried before. Furthermore, the economic advantages of the method are clearly very substantial.

Skipper et al.[23] have applied the method to an aqueous solution of $NiCl_2$ paired with $MgCl_2$. It was shown that Ni^{2+} and Mg^{2+} are isomorphic to within the limits set by the neutron method (±0.01 Å). They then performed a second-order difference experiment and deduced the M^{2+}–M^{2+} pair correlation function for the first time by X-ray methods (Figure 5). It appears from Figure 5 that there is a major discrepancy between the X-ray and the neutron determinations of $g_{NiNi}(r)$. It should be remembered, however, that large aqua cations like $[Ni(H_2O)_6]^{2+}$ interacting through Coulomb forces will give rise to a $g_{NiNi}(r)$ that is almost

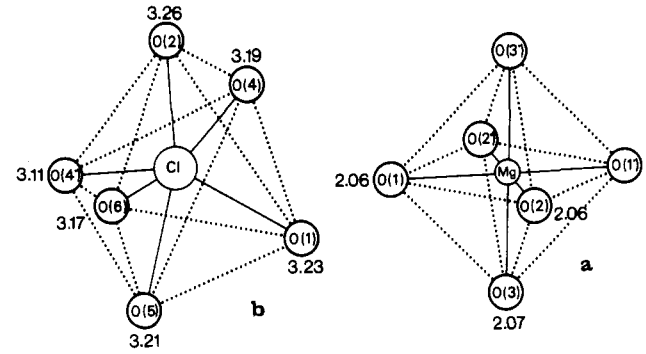

Figure 7. (a) $[Mg(H_2O)_6]^{2+}$ complex in $MgCl_2{\cdot}12H_2O$. (b) $[Cl(H_2O)_6]^-$ complex in $MgCl_2{\cdot}12H_2O$.

structureless.[22] The k-space form of $g_{NiNi}(r)$, $S_{NiNi}(k)$, is therefore dominated by the value of r_c and is relatively insensitive to the position of the first peak. As Skipper et al. show, the $S_{NiNi}(k)$ obtained by the two techniques are, within experimental error, the same, but the Fourier transform of the X-ray data is believed to be the more reliable. Both sets of data, however, allow a firm value of 4.1 ± 0.1 Å to be deduced for r_c. Studies are now in progress on a wide range of candidates for isomorphic substitution, and a systematic procedure for identifying them will be published in due course.

6. General Discussion

Much of the data shown in the tables and figures are unique and have provided new insights into the coordination chemistry involved in the study of aqueous solutions. We have, therefore, chosen three topics to discuss in some detail in order to illustrate how the method of differences can be used to deepen our understanding of the interplay between liquid-state theory, coordination chemistry, and classical crystallography.

6.1. Comparison between Crystal Hydrates and Concentrated Aqueous Solutions. A 4.35 *m* aqueous solution of $NiCl_2$ (i.e., a solution close to saturation) can be written formally as $NiCl_2{\cdot}12.8H_2O$ and would correspond to a highly hydrated solid compound. The highest hydrated $NiCl_2$ compound is, in fact, $NiCl_2{\cdot}6H_2O$, so comparison between the structure of the solution and that of the hexahydrate has little meaning. However, $MgCl_2{\cdot}12H_2O$ does exist, and its crystal structure has been fully determined.[25] Since it is now clear that aqueous solutions of $MgCl_2$ and $NiCl_2$ are isomorphic,[23] it is reasonable to make detailed structural comparison between the dodecahydrate of $MgCl_2$ and a nearly saturated solution of $NiCl_2$. In what follows, we shall use M^{2+} to represent either the Ni^{2+} or the Mg^{2+} ion.

(*a*) *The M^{2+} Environment.* The environment of Mg^{2+} in the hydrate is an undistorted octahedra (Figure 7a) with a bond length of 2.062 ± 0.003 Å. The well-coordinated character of Mg^{2+} and Ni^{2+} clearly persists in the aqueous phase, and we can conclude that the concept of a stable aqua ion in both the solid and the liquid phases is a valid one so far as Mg^{2+} and Ni^{2+} are concerned.

(*b*) *The Cl^- Environment.* As pointed out by Hunt and Friedman,[5] "quantitative information about the hydration complexes of Cl^- has been notable for its absence until the recent neutron diffraction work [of Soper et al.[2]]." It is, therefore, of considerable interest to note that the structural study of $MgCl_2{\cdot}12H_2O$ vindicates the claim[6] that the complex $[Cl(H_2O)_6]^-$ does exist although, in solution, its lifetime is less than 10 ps. The distorted structure of the complex (Figure 7b) is consistent with the weakly hydrating character[22] of the chloride ion; however, the *mean* Cl···O distance (3.20 Å) in the crystal is equal to that found for the solution (Table III).

Since the observed hydration number is less than 6 for most solutions containing the chloride ion (Table III), the reaction

$$Cl(H_2O)_6^- + {}^*H_2O \rightleftharpoons [Cl(H_2O)_5]^- + {}^*H_2O + H_2O \rightleftharpoons [Cl(H_2O)_5{}^*H_2O]^- + H_2O$$

(24) Bol, W.; Gerrits, G.; Eck, C. LvP. *J. Appl. Crystallogr.* **1970**, *3*, 486.

(25) Sasvari, K.; Jeffrey, G. A. *Acta Crystallogr.* **1966**, *20*, 875.

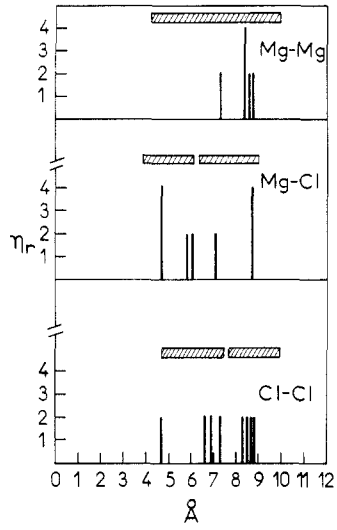

Figure 8. Histograms showing the number of neighbors η_r in crystalline $MgCl_2 \cdot 12H_2O$ of M^{2+} around M^{2+}, Cl^- around M^{2+}, and Cl^- around Cl^-. The shaded rectangles refer to the solution and show the total width of the peaks in the radial distribution functions.

probably proceeds through a dissociative mechanism with the rate constant describing water leaving the Cl^- complex greater than the rate constant describing recombination.

(*c*) *The Distribution of Ions with Respect to Ions.* The crystal structure determination of $MgCl_2 \cdot 12H_2O$ is sufficiently detailed to allow the three ion–ion distributions, M^{2+}–M^{2+}, M^{2+}–Cl^-, and Cl^-–Cl^-, to be deduced. It is clearly of interest to compare the histogram for the crystal hydrate (Figure 8) with the ion–ion radial distribution functions derived from the difference method (Figures 5 and 6). The M^{2+}–Cl^- and the Cl^-–Cl^- distribution functions shown in Figure 6 are characterized by peak positions and coordination numbers similar to those in the solid. The short Cl^-–Cl^- distance in the solid (4.70 Å) arises because two chloride ions hydrogen bond to the *same* water molecule, a situation which does not occur in the solution.[22] It is also worth noting that the closest distance of approach between Cl^- and M^{2+} is some 20% less than the first-neighbor distance in the crystal.

So far in this discussion we have emphasized the similarities between the crystal hydrate and the concentrated solution; such similarities have led some workers to the idea that concentrated solutions can be described by a "quasi-lattice", but Neilson and Enderby[22] have arrgued that such terminology should now be dropped, because the most dramatic differences between the solid and liquid become apparent when the M^{2+}–M^{2+} distribution is considered in detail. In the solution, the radial distribution function is broad and structureless and shows appreciable density in the range 4.1 Å $< r <$ 7 Å (Figure 5) where there are no corresponding solid-state distances. As Sasvari and Jeffrey[25] point out, the crystal structure is such as to ensure that the Mg^{2+} ions are as far removed from each other as possible. In solution, the need to maintain long-range order is relaxed and, as numerical simulations confirm,[22] close interactions between the hydrated cations become possible. This latter point is of considerable importance in the fundamental theory of ferrous–ferric electron exchange in aqueous solution developed by Tembe et al.[26] in which interactions at distances less than 5 Å are of particular importance. Such short interactions arise because the hydration sphere can adopt a "shoulder in armpit" configuration in which only three water molecules in each complex are between the metal centers.[27]

6.2. The Transition from Dilute Solution to the Molten Salt. Consider the following thought experiment. Imagine a dilute solution of LiCl with sufficient water present so that the hydration requirements of both Li^+ and Cl^- can be satisfied independently.

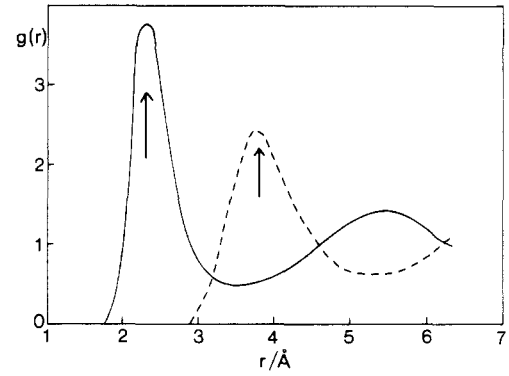

Figure 9. Radial distribution functions for molten lithium chloride (ref 28). Full curve: $g_{LiCl}(r)$; dashed curve: $g_{ClCl}(r)$. The peaks due to direct Li–Cl interactions are indicated by vertical arrows.

Then the fully hydrated ions will interact through Coulomb forces, and the number of ion pairs is, by entropy considerations, small. Now let us suppose that the water is driven off so that the solution becomes increasingly concentrated. At perhaps 5 *m* the water of hydration associated with the Li^+ ion will be shared with the Cl^- ion so that the interaction between them is of a more complicated nature than in the dilute case. At still lower water content the chloride ions will enter the inner sphere leading to direct Li^+–Cl^- interactions; finally, as all the water is driven off, we would have a molten salt in which the (small) lithium ion is surrounded by approximately four chloride ions with an arrangement close to tetrahedral.[28] We now ask, at what concentrations do these fundamental structural changes occur?

This question was addressed first by Bopp et al.[29] in a pioneering molecular dynamics study of $LiCl \cdot 4H_2O$ in the form of a solution. The results were of considerable interest because they showed that, even at these very high salt concentrations, both Cl^- and Li^+ were fully hydrated and that inner-sphere complexing in the form of ion pairs was small (that is, about one ion in ten is in contact with a counterion).

Structural studies of the hydrates of lithium salts are not common, but the structure of one hydrate with a water content on the same order as that in the Bopp et al. study, $LiClO_4 \cdot 3H_2O$, is known in detail.[30] It was found that the Li^+ is indeed fully hydrated and is of the form $[Li(H_2O)_6]^+$ with a Li–O bond length of 2.12 Å. Taken at its face value, therefore, the structure of this hydrate supports the conclusion of the molecular dynamics study.

It is, however, well-known that the perchlorate ion has little tendency to serve as a ligand; the few examples where it does coordinate to a metal ion are rather exotic (for example, the crystal $Co(CH_3SCH_2CH_2SCH_3)_2(ClO_4)_2$ studied by Cotton and Weaver[31]). The chloride ion, by contrast, frequently displaces water as a ligand as the many examples discussed by Wells[32] illustrate.

The neutron first-order and second-order difference methods have now resolved the controversy. Consider the first-order difference results for Li^+ and Cl^- in LiCl solutions shown in Tables II and III. For molalities greater than 3, both $\bar{n}_{LiO}$ and $\bar{n}_{ClO}$ begin to fall away from their "canonical" value of 6. (The value of 4 at low concentrations, often quoted for Li^+ in the literature, is incorrect; the neutron diffraction method, the most recent X-ray studies, and molecular dynamics calculations all confirm the existence of $[Li(H_2O)_6]^+$ as the dominant aqua ion in dilute solution.) The natural explanation of these data is that soluble complexes, for example, $Li(H_2O)_5Cl$ and $[Li(H_2O)_4Cl_2]^-$, begin

(26) Tembe, B. L.; Friedman, H. L.; Newton, M. D. *J. Chem. Phys.* **1982**, *76*, 1490.
(27) Friedman, H. L. In *Water and Aqueous Solutions*; Hilger: Bristol, 1986; p 117.
(28) Abernethy, G. M.; Dixon, M.; Gillan, M. J. *Philos. Mag. B* **1981**, *43*, 1113.
(29) Bopp, P.; Okadao, I.; Ohtaki, H.; Heinzinger, K. *Z. Naturforsch., A: Phys., Phys. Chem., Kosmophys.* **1985**, *40A*, 116.
(30) Chomnilpan, S.; Liminga, R.; Tellgren, R. *Acta Crystallogr., Sect. B: Struct. Crystallogr. Cryst. Chem.* **1977**, *B33*, 3954.
(31) Cotton, F. A.; Weaver, D. L. *J. Am. Chem. Soc.* **1965**, *87*, 4189.
(32) Wells, A. F. *Structural Inorganic Chemistry*; Clarendon: Oxford, 1984.

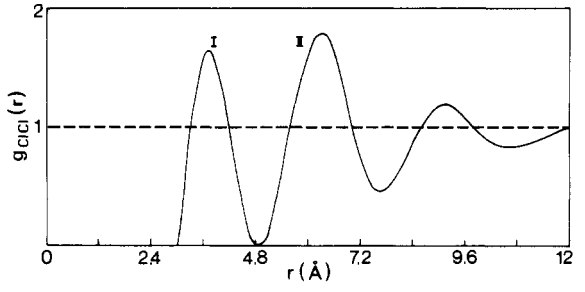

Figure 10. Pair correlation function $g_{ClCl}(r)$ for a 14.90 *m* solution of LiCl in D_2O. The two principal peaks occur at 3.75 ± 0.03 and 6.38 ± 0.03 Å, the former corresponding to the separation of chloride ions that are in direct contact with Li^+.

to be formed at molalities in excess of 3 and are present in large amounts at 10 *m* and beyond.

To establish this model conclusively, we must determine either $g_{ClCl}(r)$ or $g_{LiCl}(r)$. The presence of an appreciable fraction of, for example, $[Li(H_2O)_4Cl_2]^-$ will lead to what Copestake et al.[18] called "molten salt" peaks in both of these functions (see Figure 9). These peaks (indicated in Figure 9 by vertical arrows) arise from direct contact between Cl^- and Li^+. The chloride–chloride and the lithium–chloride peaks occur in the molten salt at ~3.8 and ~2.3 Å, respectively, and both features have in fact been observed experimentally[8,18] in concentrated aqueous solution. For example, in the $g_{ClCl}(r)$ obtained for a 14.9 *m* solution of LiCl by the second-order difference method (Figure 10), the first peak occurs at 3.75 ± 0.03 Å and is characterized by a coordination number of 2.3 ± 0.3. The fact that this peak is spread out in real space (3.0–4.8 Å, a range comparable with that observed in the molten salt) suggests that perhaps half of the coordination number arises from *intra* Cl–Cl interactions, i.e., from chloride ions within the complex $[Li(H_2O)_4Cl_2]^-$. The origin of the second peak in $g_{ClCl}(r)$ has been discussed in detail by Copestake et al.[18] and by Neilson and Enderby.[22] In a new molecular dynamics study, Tanaka et al.[33] have shown that, at a concentration corresponding to $LiCl{\cdot}3H_2O$, each Li^+ is in contact with one Cl^- ion, a substantial increase over that reported earlier for the $LiCl{\cdot}4H_2O$ solution. Theory and experiment therefore agree in concluding that ion pairing is a strong function of molarity. However, the concentration predicted by theory at which ion pairing becomes significant is quite different from that deduced from experiment, and no explanation of this discrepancy has yet been forthcoming.

A further point to note is that the experiments indicate that the hydration number of Li^+ is systematically less than that of Cl^- for concentrations greater than 3 *m*. A possible explanation of this observation is that, whereas in dilute solution the dominant species is $[Li(H_2O)_6]^{2+}$, the coordination number in the pure molten salt is 4. It is, therefore, likely that at high concentrations the value of *s* in the complex species $[Li(H_2O)_sCl_2]^-$ is nearer to 2 rather than 4 as would be the case if the coordination number for lithium remained at 6 throughout the entire composition range. It will be clearly of importance to probe the hydration number of the cation and the anion as a function of concentration for this and other solutions where complexing is expected (as, for example, in $ZnCl_2$ solutions).

6.3. Incomplete Hydration of Cations in Solution. Let *n* be the coordination number of M in the system $M_qX_p{\cdot}xH_2O$. We now define a parameter $l = x/qn$ which measures the extent to which the cations can be fully hydrated. For the *crystal* hydrate, there are, according to Wells,[32] no known exceptions to the rule that, if $l > 1$, M is fully hydrated and that the excess water is either accommodated between the $[M(H_2O)_n]^{p+}$ complexes or associated with the anions.

It is clear from diffraction studies that exceptions to this rule are found for aqueous solutions. Even for *l* values substantially in excess of unity, major differences between *n* and $\bar{n}_{MO}$ occur,

TABLE IV

cation	soln	molality	*l*	*n*	$\bar{n}_{MO}$
		9.95	0.84	6	3.3 ± 0.5
Li^+	LiCl	3.57	2.3	6	5.5 ± 0.3
		1.00	5.5	9	10.0 ± 0.6
Ca^{2+}	$CaCl_2$	2.80	2.0	9	7.2 ± 0.2
		4.49	1.2	9	6.4 ± 0.3
Cu^{2+}	$CuCl_2$	4.32	1.9	6	3.4 ± 0.2
	$Cu(ClO_4)_2$	2.00	4.2	6	4.1 ± 0.3

as the examples given in Table IV show.

The reasons for these deviations from the solid-state rule originate in the characteristic feature of the liquid state, that is, the high mobility of all of the chemical species present.

Quasi-elastic neutron scattering spectroscopy has been applied to a variety of ions,[14,34] and it is clear from these and from other studies that water molecules exchange rapidly with many cations. The values quoted for the residence times of the water molecule, τ_m (see, for example, Figure 21-9 in Cotton and Wilkinson[1]), are often too long by up to 2 or so orders of magnitude. For example, τ_m for Li^+ is now known to be $\sim 10^{-11}$ s, for Cu^{2+} τ_m is $\sim 10^{-10}$ s, and for Ca^{2+} τ_m is $\gtrsim 10^{-9}$ s. Although the data for Li^+ are not complete, a plausible interpolation of the results shown in Table IV suggests, for $l = 1$, $\bar{n}_{LiO}$ will be $\simeq 3.95$ as compared with 6 on the "Wells" rule. This almost certainly reflects the fact that the exchange mechanism is such that the equilibrium

$$[Li(D_2O)_6]^+ \rightleftharpoons [Li(D_2O)_{6-a}]^+ + aD_2O$$

lies to the right-hand side. In addition, some inner-sphere complexing by Cl^- probably occurs (Table III), but a careful study of $g_{LiCl}(r)$ by the second-order difference method is necessary before the relative importance of these two mechanisms can be fully quantified.

In the case of Cu^{2+}, where the d^9 character of the ion leads to a weakening (through a Jahn–Teller effect) of the average strength of the Cu^{2+}–H_2O bond, $\bar{n}_{CuO}$ is 4 for values of $l > 2$, even when noncoordinating ligands like ClO_4^- are involved (Table IV). When Cl^- replaces ClO_4^-, there is a tendency for inner-sphere complexing as confirmed (Table III) by the observation that the Cl^- hydration number is significantly less than 6. It is, therefore, interesting to note that $\bar{n}_{CuO}$ is somewhat less than 4 and chloride ions tend to displace some nearest-neighbor water in the inner-coordination sphere of Cu^{2+} but significantly less than had been previously supposed. There is evidence both from X-ray studies (ref 35) and from a detailed examination of the area under the second peak of $\Delta G_{Cu}(r)$ that two other water molecules are located within the r_{CuO} range 2.3–2.6 Å. A detailed review of the nature of Cu^{2+} in aqueous solution will be published by Salmon, Neilson, and Enderby in due course.

We finally consider the interesting case of Ca^{2+}. The water associated with this cation is in fast exchange on the quasi-elastic neutron time scale of $\gtrsim 10^{-9}$ s.[34] Neutron diffraction studies,[11] molecular dynamics,[36] quantum chemistry,[37] and X-ray diffraction[38] have established that, at low salt concentration, the hydration number of Ca^{2+} is ~10. The interesting result shown in Table IV is the extent to which the hydration number of Ca^{2+} depends on concentration, even though $l > 1$. It is true that the coordination number of Ca^{2+} varies from 6 to 9 in crystal hydrates,[32] but here the concentration scale of the water content is entirely different. The reduction in $\bar{n}_{CaO}$ from ~10 to ~6 (Table IV) cannot be simply a matter of inner-sphere complexing by Cl^- because the chloride hydration number in 4.49 *m* solution is 5.8 ± 0.2, i.e., close to the canonical value. Two possibilities remain:

(33) Tanaka, K.; Ogita, N.; Tamura, Y.; Okada, I.; Ohtaki, H.; Pálinkás, G.; Spohr, E.; Heinzinger, K. *Z. Naturforsch., A: Phys., Phys. Chem., Kosmophys.* **1987**, *42A*, 29.

(34) Hewish, N. H.; Enderby, J. E.; Howells, W. S. *J. Phys. C: Solid State Phys.* **1983**, *16*, 1777. Salmon, P. S. *J. Phys. C: Solid State Phys.* **1987**, *20*, 1573.

(35) Magini, M. *J. Chem. Phys.* **1981**, *74*, 2523.

(36) Bounds, D. G. *Mol. Phys.* **1985**, *54*, 1335.

(37) Ortega-Blake, I.; Novaro, O.; Lés, A.; Rybak, S. *J. Chem. Phys.* **1982**, *76*, 5405.

(38) Probst, M. M.; Radnai, T.; Heinzinger, K.; Bopp, P.; Rode, B. M. *J. Phys. Chem.* **1985**, *89*, 753.

the coordination number of Ca^{2+} is indeed strongly concentration dependent in the solution and for $l \sim 1$ is as low as six; alternatively, Ca^{2+}–Ca^{2+} interactions occur within the inner sphere, leading to a reduction in $\bar{n}_{CaO}$ directly. We think this latter suggestion is implausible; it is, however, of interest that, of the five molten divalent metal chlorides so far studied, a short cation–cation bond length occurs *only* in molten $CaCl_2$. Biggin and Enderby[39] found that $\bar{r}_{CaCa}$ was 3.58 Å and, in spite of the double charge on the calcium ion, was some 4% *less* than $\bar{r}_{ClCl}$ (3.73 Å).

(39) Biggin, S.; Enderby, J. E. *J. Phys. C: Solid State Phys.* **1981**, *14*, 3577.

Once again, the importance of determining the cation–cation distribution function in the solution is clear, but the technology for doing this needs to be further developed and refined.

Acknowledgment. The work reported in this article has been generously supported by the United Kingdom Science & Engineering Research Council. The staff at the ILL, Grenoble, France, particularly Pierre Chieux and Adrian Barnes, are thanked for their help with the experiments. J.E.E. acknowledges many helpful discussions with H. L. Friedman which were made possible by the award of a NATO travel grant (RG 125/80). We also thank Janet Wallace for producing an excellent typed version of our handwritten manuscript.

ARTICLES

The Temperature Invariance of the NO_3 Absorption Cross Section in the 662-nm Region

C. A. Cantrell,* J. A. Davidson, R. E. Shetter, B. A. Anderson,† and J. G. Calvert

National Center for Atmospheric Research,‡ Boulder, Colorado 80307 *(Received: December 29, 1986; In Final Form: May 19, 1987)*

Several laboratory measurements of the absorption cross section of NO_3 in the visible region near 662 nm have been reported. Two recent studies have indicated a possible temperature dependence for this cross section. This paper describes the results of measurements of the peak absorption cross section ($\sigma^{662}_{NO_3}$) and the integrated area ($\sigma^{I}_{NO_3}$) of the 662-nm NO_3 band as a function of temperature from 215 to 348 K, using Fourier transform spectroscopy. Within the error limits of this study, no dependence of $\sigma^{662}_{NO_3}$ or $\sigma^{I}_{NO_3}$ on temperature could be seen. It is recommended that temperature-independent values of 2.08 (±0.38) × 10^{-17} cm^2 $molecule^{-1}$ be used for the peak cross section of the 662-nm band (15 106 cm^{-1}) and 1.95 (±0.18) × 10^{-15} cm^2 $molecule^{-1}$ cm^{-1} be used for the integrated band intensity (14 910–15 290 cm^{-1}). When possible, the integrated area of this band should be used to quantify NO_3 because there is less uncertainty in the integrated band strength as compared to the peak height.

Introduction

The NO_3 radical has been identified as a key reactant in the NO_x chemistry of the atmosphere and, as such, has been the subject of a number of laboratory and field studies. In many of these studies the concentration of NO_3 has been determined through its absorption maximum near 662 nm. Since the accuracy of the NO_3 concentration determination is directly related to this absorption cross section maximum ($\sigma^{662}_{NO_3}$), it is crucial that it be accurately determined.

The visible absorption spectrum of NO_3 was first recorded by Jones and Wolf[1] and has subsequently been shown by Ramsey[2] and by Marinelli et al.[3] to be completely free of rotational structure even at very high resolution. The anomalously long lived fluorescence observed[4-6] and the photodissociation quantum yield of zero at wavelengths longer than about 630 nm[7,8] rule out predissociation in explanation of the diffuse spectrum. Nelson et al.[6] have suggested that this diffuseness and the long lifetime of the excited state can be attributed to mixing of the excited-state electronic levels with high vibronic levels of the ground state.

Schott and Davidson,[9] using thermal decomposition of N_2O_5 as the NO_3 source, were the first to determine an NO_3 absorption cross section. Subsequent determinations have used a variety of NO_3 sources including $NO_x + O_3$,[3,8,10,11] $F + HNO_3$,[12-15] and $Cl + ClONO_2$.[13,15,16] The most recent measurements of ($\sigma^{662}_{NO_3}$) are

TABLE I: Results of Previous Determinations of the Cross Section for the Peak of the NO_3 Band near 662 nm ($\sigma^{662}_{NO_3}$) and the Integrated Cross Section from 14 910 and 15 290 cm^{-1} ($\sigma^{I}_{NO_3}$)

ref	source	temp, K	$\sigma^{662}_{NO_3}$ [a]	$\sigma^{I}_{NO_3}$ [b]
10	$NO_x + O_3$	298	1.48	1.83
8	$NO_x + O_3$	298	1.71	1.99
11	$NO_x + O_3$	298	1.21	2.06
3	$NO_x + O_3$	298	1.90	2.02
12	$F + HNO_3$ (DF[c])	298	1.78	1.88
16	$Cl + ClONO_2$ (P[d])	298	1.63	
13	$F + HNO_3$ (DF), $Cl + ClONO_2$ (P)	298	1.85	1.82
14	$F + HNO_3$ (DF)	298	1.90	1.94
14	$F + HNO_3$ (DF)	240	2.31	2.22
14	$F + HNO_3$ (DF)	220	2.71	2.42
15	$Cl + ClONO_2$ (FP[e])	298	2.28	
15	$Cl + ClONO_2$ (FP)	250	2.62	
15	$Cl + ClONO_2$ (FP)	230	2.70	
15	$F + HNO_3$ (DF)	298	1.83	
this work	$NO_x + O_3$	215–348	2.06	2.02

[a] cm^2 $molecule^{-1}$, ×10^{17}. [b] cm^2 $molecule^{-1}$ cm^{-1}, ×10^{15}. [c] Discharge flow. [d] Photolysis. [e] Flash photolysis.

† Present address: Department of Chemistry, University of Chicago, Chicago, IL.

‡ The National Center for Atmospheric Research is funded by the National Science Foundation.

(1) Jones, E. J.; Wulf, O. R. *J. Chem. Phys.* **1937**, *5*, 873.

0022-3654/87/2091-5858$01.50/0